

000 001 002 003 004 005 006 007 008 009 010 011 012 013 014 015 016 017 018 019 020 021 022 023 024 025 026 027 028 029 030 031 032 033 034 035 036 037 038 039 040 041 042 043 044 045 046 047 048 049 050 051 052 053 IC-CUSTOM: DIVERSE IMAGE CUSTOMIZATION VIA IN-CONTEXT LEARNING

Anonymous authors

Paper under double-blind review

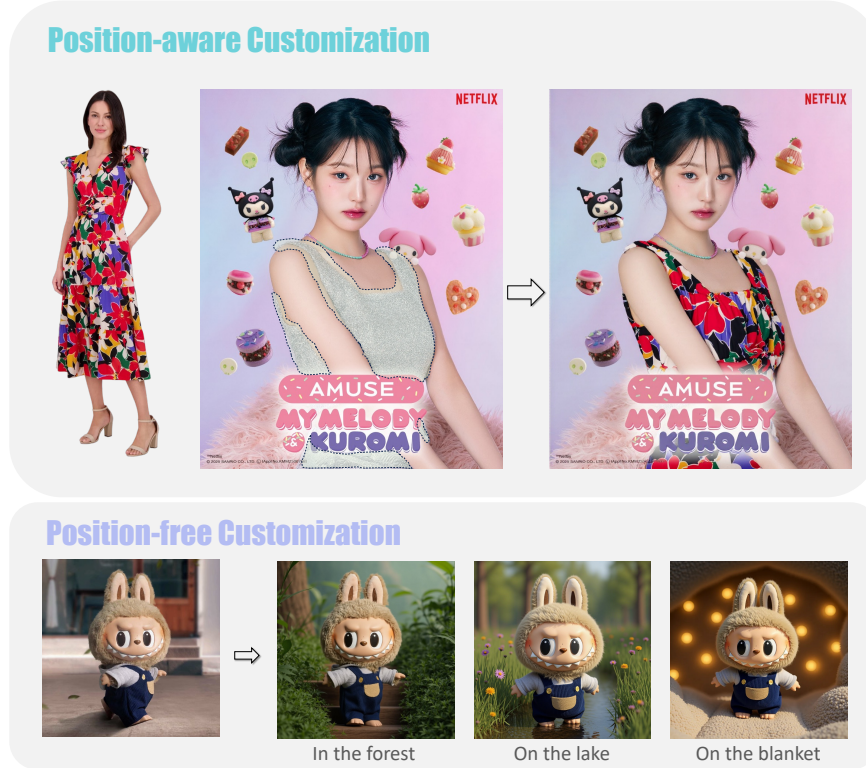


Figure 1: **Visualization of *IC-Custom* results.** Our method supports diverse image customization scenarios, including position-aware (location-specified editing conditioned on a mask) and position-free (ID-consistent generation guided by text) customization.

ABSTRACT

Image customization, a crucial technique for industrial media production, aims to generate content that is consistent with reference images. However, current approaches conventionally separate image customization into position-aware and position-free customization paradigms and lack a universal framework for diverse customization, limiting their applications across various scenarios. To overcome these limitations, we propose *IC-Custom*, a unified framework that seamlessly integrates position-aware and position-free image customization through in-context learning. *IC-Custom* concatenates reference images with target images to a polyptych, leveraging DiT’s multi-modal attention mechanism for fine-grained token-level interactions. We propose the In-context Multi-Modal Attention (ICMA) mechanism, which employs learnable task-oriented register tokens and boundary-aware positional embeddings to enable the model to effectively handle diverse tasks and distinguish between inputs in polyptych configurations. To address the data gap, we curated a 12K identity-consistent dataset with 8K real-world and 4K high-quality synthetic samples, avoiding the overly glossy, oversaturated look typical of synthetic data. *IC-Custom* supports various industrial applications, including try-on, image insertion, and creative IP customization. Extensive evaluations

054
055
056
057
058
059

on our proposed *ProductBench* and the publicly available *DreamBench* demonstrate that *IC-Custom* significantly outperforms community workflows, closed-source models, and state-of-the-art open-source approaches. *IC-Custom* achieves about 73% higher human preference across identity consistency, harmony, and text alignment metrics, while training only 0.4% of the original model parameters.

060
061

1 INTRODUCTION

062
063
064
065
066
067

Image customization, which ensures that generated content remains consistent with the identity of reference images, has enabled applications such as image insertion (Chen et al., 2024a;b; Mao et al., 2025; Song et al., 2025), IP creation (Ruiz et al., 2023b; Ye et al., 2023b; Tewel et al., 2024; Tan et al., 2024; Mou et al., 2025), and visual try-on (Wang et al., 2024; Guo et al., 2025; Xu et al., 2025). These capabilities are vital for industrial media production, supporting consistent content creation across diverse visual contexts.

068
069
070
071
072
073
074
075
076
077

Early image customization methods (Ruiz et al., 2023a; Gal et al., 2022; Avrahami et al., 2023) relied on per-instance optimization, which was time-consuming. Subsequent approaches (Ye et al., 2023a; Chen et al., 2024b;a) added control branches to pre-trained diffusion models to inject identity information from reference images. However, these methods were constrained by model architecture and scalability issues, resulting in suboptimal performance. Recently, by leveraging the long-range modeling inductive bias of DiT architectures (Peebles & Xie, 2023b; Esser et al., 2024b; Labs, 2024a), image conditions can be directly input as sequences, interacting with noisy tokens through multi-modal attention mechanisms, without the need for additional branches. This enables image customization methods to exhibit powerful emergent capabilities (Song et al., 2025; Mou et al., 2025; Labs, 2024b;c; Tan et al., 2024; Mao et al., 2025).

078
079
080
081
082
083
084
085
086
087
088
089
090
091
092

Despite these advances, existing methods still face significant challenges in maintaining consistent identity across diverse user requirements and customization scenarios (see Tab. 1): (1) They typically treat image customization as two separate tasks. In *position-aware* customization, an reference identity is inserted into masked regions of a fill-in image. In *position-free* customization, identity-consistent images are generated from text prompts. (2) They provide limited support for diverse mask types, often confusing user-drawn with precise masks, e.g., treating coarse hand-drawn regions as exact boundaries. These limitations hinder the development of unified frameworks capable of flexibly handling diverse customization requirements, forcing separate models for each scenario and limiting the development of robust, comprehensive identity representations.

093
094
095
096
097
098
099
100
101
102
103
104
105
106
107

To this end, we propose *IC-Custom*, a unified framework that seamlessly integrates position-aware and position-free image customization, enabling flexible and identity-consistent customization across diverse scenarios (see Fig. 1). Specifically, we first employ a diptych format by concatenating the reference identity image with the fill-in image (either partially or fully masked), yielding a unified representation that allows the model to handle diverse customization settings within a single framework. Building on DiT’s multi-modal attention, we further introduce a novel In-Context Multi-Modal Attention (ICMA) module that more effectively transfers identity information from the reference image to the fill-in image and enables comprehensive customization across diverse scenarios. The ICMA module features two key innovations: (1) Three types of learnable, task-oriented register tokens to specify the customization type—position-aware customization (with precise or user-drawn masks) and position-free customization—allowing the model to adapt its behavior based on user requirements. (2) Two types of learnable positional embeddings to represent spatial relationships: Reference Embeddings (RE) for the reference identity image and Fill Embeddings (FE) for the fill-in image, helping the model clearly differentiate input boundaries in the diptych format.

To enable effective training of our unified framework, we curated a high-quality dataset *CustomData*, consisting of both real-world and synthetic samples. Specifically, we curated 8K identity-consistent

Table 1: Comparison of *IC-Custom* with previous image customization methods (Labs, 2024b;c; Tan et al., 2024; Song et al., 2025; Mou et al., 2025; Hurst et al., 2024b). The checkmarks and crosses indicate task compatibility.

Model	Position-aware		Position-free
	precise	user-drawn	
FLUX.1 workflow	✓	✓	✗
OminiCtrl	✗	✗	✓
Insert Anything	✓	✓	✗
DreamO	✗	✗	✓
GPT-4o	✗	✗	✓
<i>IC-Custom</i>	✓	✓	✓

108 diptychs from real-world sources and an additional 4K synthetic diptychs, resulting in a total of 12K
 109 diptychs. This comprehensive dataset enables our model to learn robust identity representations
 110 across diverse contexts and viewpoints, while also addressing the limitations of previous methods
 111 that overly rely on synthetic data and often produce artificial-looking results.

112 To extensively evaluate the performance of our method, we use *ProductBench* and *Dream-
 113 Bench* (Ruiz et al., 2023a) to assess both position-aware and position-free customization capabilities.
 114 *ProductBench* is our manually curated benchmark for position-aware customization, consisting of
 115 40 identity-consistent images with an even distribution of rigid and non-rigid objects, along with
 116 their corresponding precise and user-drawn masks. We also use *DreamBench* to evaluate position-
 117 free customization performance. Extensive subjective and objective evaluations demonstrate that
 118 *IC-Custom* outperforms community workflows, the closed-source GPT-4o (March 25, 2025), and
 119 state-of-the-art open-source approaches. Notably, *IC-Custom* achieves a 73% higher human prefer-
 120 ence across identity consistency, harmony, and text alignment metrics, while training only 0.3% of
 121 the parameters of the pre-trained FLUX model.

122 In summary, our contributions are as follows:
 123

- 124 • We propose a unified framework that seamlessly integrates position-aware and position-free image
 125 customization via in-context formulation.
- 126 • We introduce the ICMA module, which enables flexible image customization through learnable
 127 task-oriented register tokens and boundary-aware positional embeddings.
- 128 • We curate a dataset from real-world sources, addressing the limitations of existing methods that
 129 rely on synthetic data, which often produce artificial-looking results.
- 130 • We demonstrate that our method outperforms existing approaches across a range of metrics, sur-
 131 passing community workflows, closed-source models, and state-of-the-art open-source methods.

132 2 PRELIMINARIES

133 **MM-DiT Architecture.** Recent state-of-the-art generative diffusion models, such as SD3 (Esser
 134 et al., 2024b) and FLUX (Labs, 2024a), leverage the MM-DiT architecture (Peebles & Xie, 2023a),
 135 which integrates a Multi-modal Attention (MMA) mechanism with Rotary Position Embedding
 136 (RoPE) as a central component. This design enables the concurrent processing of noisy image
 137 tokens $X_t \in \mathbb{R}^{n \times d}$ and text tokens $C_T \in \mathbb{R}^{l \times d}$, as shown in Eq. 1.

$$140 \quad \text{MMA}([X_t; C_T]) = \text{softmax} \left(\frac{\mathcal{R}(Q) \cdot \mathcal{R}(K)^\top}{\sqrt{d}} \right) \mathcal{R}(V). \quad (1)$$

141 Here, Q , K , and V are derived from the projection of the concatenated input $[X_t; C_T] \in \mathbb{R}^{(n+l) \times d}$,
 142 with the operator \mathcal{R} applying RoPE to Q and K to encode positional information.

143 **Flow Matching.** The model is trained within the Rectified Flow (RF) (Liu et al., 2022). The
 144 Continuous Normalizing Flow (CNF) is formalized as the following ODE:
 145

$$146 \quad \frac{d}{dt} X_t = v(X_t, t) dt = X_1 - X_0, \quad \forall t \in [0, 1]. \quad (2)$$

147 Here, given a clean latent variable $X_0 \sim p_{\text{data}}$ and a Gaussian noise sample $X_1 \sim \mathcal{N}(0, 1)$, X_t is
 148 constructed via linear interpolation:
 149

$$150 \quad X_t = tX_1 + (1 - t)X_0, \quad \forall t \in [0, 1]. \quad (3)$$

151 Subsequently, the Conditional Flow Matching (CFM) loss (Lipman et al., 2023) is employed to train
 152 a velocity field prediction model v_Θ :

$$153 \quad \mathcal{L}_{\text{CFM}} = \mathbb{E}_{t \sim p(t), X_1 \sim \mathcal{N}(0, 1), (X_0, C_T) \sim p_{\text{data}}} \left[\|v_\Theta(X_t, C_T, t) - (X_1 - X_0)\|_2^2 \right]. \quad (4)$$

154 Here, t is sampled from a *Logit-Normal Distribution* (Esser et al., 2024a) with the probability den-
 155 sity function $p(t) = \frac{\exp(-0.5 \cdot (\text{logit}(t) - \mu)^2 / \sigma^2)}{\sigma \sqrt{2\pi} \cdot (1-t) \cdot t}$, where $\text{logit}(t) = \log \frac{t}{1-t}$. From the Logit-Normal
 156 Distribution definition, $Y = \text{logit}(t) \sim \mathcal{N}(\mu, \sigma)$, with $\mu = 0$ and $\sigma = 1$ under the RF.

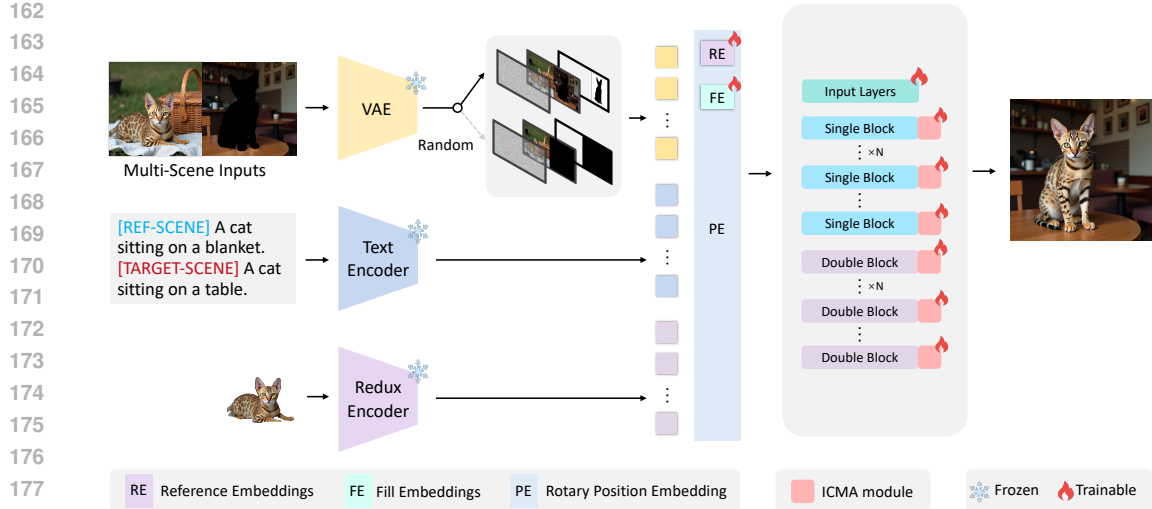


Figure 2: **Model overview.** (1) Our model takes in-context diptych inputs together with redux embeddings and text prompts. (2) During training, it randomly chooses to mask either the entire fill-in image (position-free customization) or only partial regions (position-aware customization) to produce diverse in-context latents. (3) The ICMA module, equipped with task-oriented register tokens and boundary-aware positional embeddings (see Sec. 3.2), is integrated into the architecture. We train LoRA adapters on the ICMA module while unfreezing the input layers.

DiT-based Image Customization Methods Recent state-of-the-art DiT-based image customization methods (Chen et al., 2024c; Mao et al., 2025; Wu et al., 2025; Song et al., 2025; Mou et al., 2025), integrate reference image conditions directly into the input via concatenation, instead of using additional network branches. This method unifies reference and other conditions into a single sequence, improving integration during flow matching. However, these methods typically train position-aware and position-free customization tasks separately, without explicitly addressing their potential unification. In position-aware tasks, the identity’s location is specified using a mask, while position-free tasks leverage textual guidance to generate identity-consistent content. For instance, ACE++ (Mao et al., 2025) and OmniControl (Tan et al., 2024) train separate LoRA adapters, InsertAnything (Song et al., 2025) is specifically trained for position-aware tasks, and DreamO (Mou et al., 2025) and UNO (Wu et al., 2025) are designed for position-free tasks.

3 METHOD

As shown in Fig. 2, we introduce *IC-Custom*, a novel approach that presents a unified framework for comprehensive image customization, as detailed in Sec. 3.1. At its core, *IC-Custom* leverages In-Context Multi-Modal Attention (ICMA) to effectively adapt to diverse customization scenarios, as described in Sec. 3.2. Additionally, we curate a high-quality dataset for comprehensive customization tasks, sourced from both real-world and synthetic data, with image resolutions exceeding 800×800 pixels, as outlined in Sec. 3.3.

3.1 IN-CONTEXT DIPTYCH CUSTOMIZATION

Motivation. Formally, position-aware customization can be framed as a reference-guided image filling task, represented as $p(\hat{X} | C_I, C_{I'}, M)$, where \hat{X} denotes the customized output, C_I denotes the reference identity image, $C_{I'}$ represents the image to be filled, and M denotes the mask specifying the filling position. In contrast, position-free customization is viewed as a reference-guided text-to-image task, formalized as $p(\hat{X} | C_I, C_T)$. Since position-free customization can be regarded as a special case of image filling where M and $C_{I'}$ are set to zero, we unify both paradigms under the formulation $p(\hat{X} | C_I, C_{I'}, M, C_T)$.

216 **Diptych Framework and Training Strategy.** Based on the unified formulation above, we introduce an in-context¹ diptych format to unify diverse input conditions and support this paradigm. 217 Specifically, we concatenate the reference identity image C_I with the fill-in image $C_{I'}$ in a diptych 218 layout, then encode them jointly as tokens to enforce simultaneous modeling and generation. The 219 model is trained with the following CFM loss:

$$221 \quad \mathcal{L}_{\text{CFM}} = \mathbb{E}_{t \sim p(t), X_1 \sim \mathcal{N}(0,1), (X_0, C_T) \sim p_{\text{data}}} \left[\|v_{\Theta}([X_t, X_0^m, M], C_T, t) - (X_1 - X_0)\|_2^2 \right], \quad (5)$$

222 where $X_0 = [C_I; C_{I'}]$ denotes the width-wise diptych concatenation of the reference identity image 223 and the fill-in image, X_t is computed according to Eq. 3, and $X_0^m = X_0 \odot M$, with \odot indicating 224 element-wise multiplication. Here, $[X_t, X_0^m, M]$ represents the channel-wise concatenation of these 225 three components. The text condition C_T provides scene descriptions for both the reference identity 226 image and the fill-in image, separated by the placeholders [REF-SCENE] and [TARGET-SCENE]. 227 Notably, during training, instead of requiring triplets $(C_I, C_{I'}, \hat{X})$, where $C_{I'}$ and \hat{X} typically differ 228 in identity, we use two images of the same identity and set $\hat{X} = C_{I'}$, enabling the model to predict 229 $C_{I'}$ conditioned on M and X_0^m ; hence Eq. 5 defines $X_0 = [C_I; C_{I'}]$ rather than $X_0 = [C_I; \hat{X}]$. 230

231 Based on this formulation, once paired data $\{C_I, C_{I'}, M, C_T\}$ are available, the model can be trained 232 in two complementary modes without collecting separate datasets or designing distinct model 233 structures. Specifically, setting $C_{I'}$ and M to zero (i.e., a global mask) corresponds to position-free 234 customization, while using nonzero (localized) masks for $C_{I'}$ and M enables position-aware cus- 235 tomization. Thus, a single paired dataset suffices to support both capabilities through simple varia- 236 tions in training inputs.

237 In implementation, as shown in Fig. 2, we use a VAE (Kingma et al., 2013b) to encode the input 238 diptych, while T5 (Raffel et al., 2020) and CLIP (Radford et al., 2021) serve as text encoders for 239 the text prompts. Optionally, FLUX.1 Redux (Labs, 2024c) is employed to further encode identity 240 information. The resulting representations are then fed into DiT blocks equipped with the ICMA 241 module (see Sec. 3.2) for flow matching.

242 3.2 IN-CONTEXT MULTI-MODAL ATTENTION

243 **Challenges.** Although our pipeline seamlessly adapts to diverse customization settings, it still 244 faces several challenges. (1) *Task-type ambiguity*: for example, under position-aware customization 245 settings, the model often misinterprets user-drawn masks as precise boundaries, generating content 246 that fully fills and strictly follows the mask shape. (2) *Image-boundary confusion*: in diptych pre- 247 diction settings (Eq. 5), the model struggles to differentiate between reference and target regions, 248 leading to undesirable edge artifacts.

249 **Proposed ICMA.** To address these issues, we propose In-Context Multi-Modal Attention module 250 (ICMA), a variant of the multi-modal attention mechanism. As illustrated in Fig. 3 (a), ICMA 251 incorporates two key design innovations: (1) *learnable task-oriented register tokens* to explicitly 252 indicate the customization type (precise masks, user-drawn masks, or position-free); and (2) *learnable 253 boundary-aware positional embeddings*—comprising Reference Embeddings (RE) and Fill Embed- 254 dings (FE)—to encode spatial relationships between the reference identity image and the fill-in 255 image. Formally, the ICMA mechanism operates as follows:

$$256 \quad \begin{aligned} \mathcal{P}(x) &= x + [\mathcal{E}_R; \mathcal{E}_F] + \mathcal{R}(x), \\ 257 \quad Q &= [\mathcal{P}(Q_I); Q_T + \mathcal{R}(Q_T)], \\ 258 \quad K &= [\mathcal{P}(K_I); K_T + \mathcal{R}(K_T)]; \mathbf{r}_i, \\ 259 \quad V &= [V_I; V_T; \mathbf{r}_i], \\ 260 \quad h' &= \text{MHA}(Q, K, V), \end{aligned} \quad (6)$$

261 where $[;]$ denotes diptych concatenation, $\mathcal{R}(\cdot)$ denotes rotary position encoding (Su et al., 2024); 262 $Q_I, K_I, V_I \in \mathbb{R}^{n \times d}$ and $Q_T, K_T, V_T \in \mathbb{R}^{l \times d}$ are the query, key, and value matrices for image 263 and text tokens, respectively; $\mathcal{E}_R, \mathcal{E}_F$ are the learnable Reference and Fill embeddings; $\mathbf{r}_i \in \mathbb{R}^{m \times d}$ 264 denotes the i -th learnable task-oriented register token; and $\text{MHA}(\cdot)$ is the Multi-Head Attention 265 operation. Our proposed ICMA module replaces the multi-modal attention layers in both the double- 266 block and single-block components of the original FLUX.1 MM-DiT architecture (Labs, 2024a).

267 ¹Here, “in-context” refers to concatenating images and jointly conditioning on their captions.

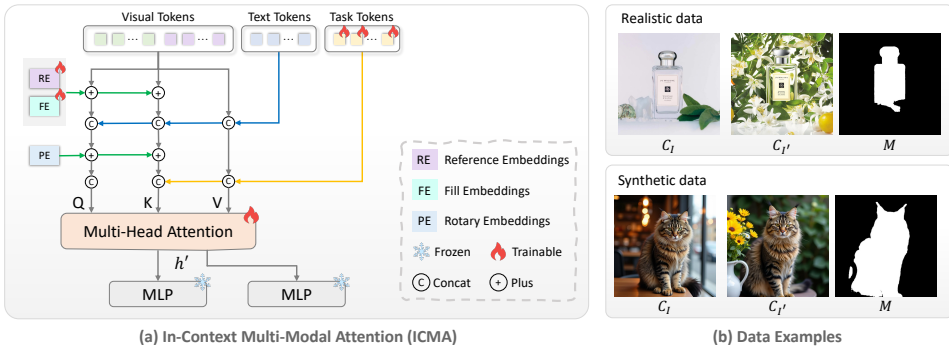


Figure 3: (a) **In-Context Multi-Modal Attention (ICMA)**. ICMA incorporates learnable task-oriented register tokens and boundary-aware positional embeddings (RE, FE) into the multi-modal attention of MM-DiT (Peebles & Xie, 2023a) to specify customization types and delineate input boundaries. (b) **Training data examples**. High-quality identity-consistent quadruples $\{C_I, C_{I'}, M, C_T\}$ from real-world and synthetic data; for clarity, text descriptions C_T are omitted.

3.3 IN-CONTEXT CUSTOMIZATION DATA CURATION

Data Collection. The scarcity of high-quality customization data remains a critical bottleneck in developing robust customization models. Existing approaches (Tan et al., 2024; Wu et al., 2025; Li et al., 2025) rely predominantly on synthetic data for training; however, such data often struggles to preserve identity consistency and photorealistic quality, thereby limiting model effectiveness.

To address this challenge, we introduce *CustomData*, a high-quality customization dataset designed for both authenticity and diversity. We curate nearly 8K identity-consistent realistic image pairs from e-commerce platforms, covering real-world scenarios such as clothing try-on, cosmetics, furniture, electronics, accessories, home decor, and personal care products, with resolutions ranging from 800×800 to 3000×3664 pixels. To further enrich the dataset and extend coverage beyond commercial products, we add 4K high-quality, identity-consistent synthetic pairs carefully filtered from the SynCD 1024×1024 subset (Kumari et al., 2025), resulting in a comprehensive dataset of 12K $\{C_I, C_{I'}, M, C_T\}$ samples (see Fig. 3(b) for visualization; symbol definitions in Sec. 3.1).

Data Processing. Our filtering process applies three rules: (1) exclude items whose DINov2 (Oquab et al., 2023) feature similarity between C_I and $C_{I'}$ is below 0.2; (2) discard pairs composed entirely of blank-background images; and (3) ensure $C_{I'}$ is not a blank-background image. These rules improve identity consistency and reduce ambiguity. We then use Qwen-VL2.5 (Bai et al., 2025) to auto-generate captions for *CustomData* (system prompt in Appendix Sec. J) and Grounded SAM (Ren et al., 2024) to obtain ground-truth masks, while randomly generating user masks under predefined rules to support model training (see Appendix Sec. L for details).

4 EXPERIMENTS

4.1 EXPERIMENTS SETUP

Implementation Details. *IC-Custom* builds on the pre-trained text-to-image model FLUX.1-Fill (Labs, 2024b). We train LoRA (Hu et al., 2022) (rank 64) on the first 10 layers of both single and double blocks, while directly fine-tuning the image and text input layers. In total, only 49.26M parameters are trainable—just 0.4% of the original FLUX model’s 12B parameters (19 double and 38 single blocks). Unlike prior methods (Song et al., 2025; Mou et al., 2025) that train LoRA on all layers (e.g., DreamO (Mou et al., 2025) trained 707M parameters), our approach drastically cuts training cost. The model is optimized on our 12K dataset for 20K iterations using AdamW (Loshchilov & Hutter, 2017) with a learning rate of 5×10^{-5} and a batch size of 4. To handle diverse resolutions, we employ a data-bucketing strategy that groups samples by size (e.g., 800×800 , 1024×1024 , 1024×1280 , 1280×1280 , 1504×1504) so each batch has uniform input dimensions. We also present a web application and inference pipeline in Appendix M.

324
 325 **Table 2: Quantitative results on position-aware and position-free image customization.** Evaluation
 326 on *ProductBench* (precise/user-drawn masks) and *DreamBench* shows that *IC-Custom* consis-
 327 tently outperforms existing methods across all objective metrics (higher is better \uparrow). Baselines:
 328 FLUX.1 workflow (Labs, 2024b;c), OminiCtrl/DreamO/Insert Anything (Tan et al., 2024; Mou
 329 et al., 2025; Song et al., 2025), GPT-4o (Hurst et al., 2024b).

Method	ProductBench						DreamBench		
	Precise Mask			User-drawn Mask			Position-free		
	DINO-I \uparrow	CLIP-I \uparrow	CLIP-T \uparrow	DINO-I \uparrow	CLIP-I \uparrow	CLIP-T \uparrow	DINO \uparrow	CLIP \uparrow	CLIP-T \uparrow
FLUX.1 workflow	60.80	81.66	31.13	62.26	81.60	31.29	—	—	—
OminiCtrl	57.93	76.06	31.31	—	—	—	48.29	75.85	36.82
DreamO	62.98	78.86	31.25	—	—	—	57.69	76.33	36.24
Insert Anything	62.71	81.65	31.24	61.21	81.75	31.44	—	—	—
GPT-4o	61.40	78.53	30.72	62.05	79.87	30.58	54.31	77.38	36.33
IC-Custom (Ours)	63.14	81.92	31.75	63.28	81.95	31.80	65.67	83.19	36.88

330
 331 **Table 3: (a) Human-study results on image customization quality (higher is better). (b) Abla-**
 332 **tion studies on ProductBench.** Abbreviations: Zero-shot = zero-shot inference without fine-tuning;
 333 w/o IL = without training Input Layers; w/o RD = without using Real Data for training; w/o UM =
 334 without using User-drawn Mask for training; w/o TR = without Task-oriented Register tokens; w/o
 335 PE = without Boundary-aware Positional Embeddings.

Method	(a) Human-study results			(b) Ablation on ProductBench					
	Consistency \uparrow	Harmony \uparrow	Text Alignment \uparrow	Precise Mask			User-drawn Mask		
				DINO-I \uparrow	CLIP-I \uparrow	CLIP-T \uparrow	DINO-I \uparrow	CLIP-I \uparrow	CLIP-T \uparrow
FLUX.1 workflow	3.2%	5.3%	—	55.49	77.55	31.24	57.63	79.84	31.20
OminiCtrl	1.5%	2.1%	6.3%	62.00	81.52	31.36	62.13	81.33	31.64
DreamO	5.4%	3.2%	10.1%	62.38	81.81	31.62	62.71	81.85	31.22
Insert Anything	6.8%	6.5%	—	62.65	81.82	31.58	61.30	81.28	31.64
GPT-4o	4.6%	7.5%	21.4%	63.00	81.42	31.43	63.07	81.44	31.33
Ours	78.5%	75.4%	62.2%	62.99	81.31	31.42	63.08	81.40	31.30

351
 352 **Benchmarks.** To assess our model’s performance in both position-aware and position-free cus-
 353 tomization settings, we evaluate on our proposed *ProductBench* and the open-source *Dream-*
 354 *Bench* (Ruiz et al., 2023a) benchmark. *ProductBench* contains 40 high-quality, identity-consistent
 355 items with resolutions exceeding 1024×1024 pixels. Each item includes paired images and cor-
 356 responding masks, with no overlap with our training data. We use SAM (Kirillov et al., 2023)
 357 to annotate precise masks and manually create user-drawn masks. The dataset is evenly divided
 358 into rigid and non-rigid categories, covering diverse domains such as clothing try-on, accessories,
 359 bags, furniture, toys, and perfume, specifically designed to evaluate position-aware customization.
 360 *DreamBench* comprises 30 items, each with 5–6 identity-consistent images and used to evaluate
 361 position-free customization. We take the first image of each item as the reference. Additionally, we
 362 use Qwen-VL2.5 (Bai et al., 2025) to generate in-context textual descriptions for both benchmarks.
 363 For *ProductBench*, we directly prompt it to caption the diptych input, whereas for *DreamBench* we
 364 prompt it to creatively generate new scene descriptions. (see Appendix Sec. K for details)

365 **Metrics.** Follow established methods (Ruiz et al., 2023a; Wu et al., 2025), we consider 3 objective
 366 evaluation metrics across two aspects: identity consistency, and text alignment.

367 • **Identity Consistency:** We calculate the DINO-I Score (Oquab et al., 2023) and CLIP-I (Radford
 368 et al., 2021) Score between reference images and generated images to assess identity preservation.
 369 • **Text Alignment:** We use the CLIP-T score (Radford et al., 2021) to evaluate the model’s
 370 instruction-following ability.

371 We also incorporate subjective evaluation metrics: identity consistency, harmony, and text alignment
 372 to assess the performance of customization models.

373 **Baselines.** We compare our approach against several strong baselines, including the community
 374 FLUX.1 workflow (FLUX.1-Fill with FLUX.1-Redux) (Labs, 2024b;c), state-of-the-art DiT-based
 375 open-source methods OminiCtrl (Tan et al., 2024), DreamO (Mou et al., 2025), and Insert Any-
 376 thing (Song et al., 2025), as well as the commercial system GPT-4o (Hurst et al., 2024a) (March 25,
 377 2025). Among them, FLUX.1 workflow and Insert Anything are primarily designed for position-

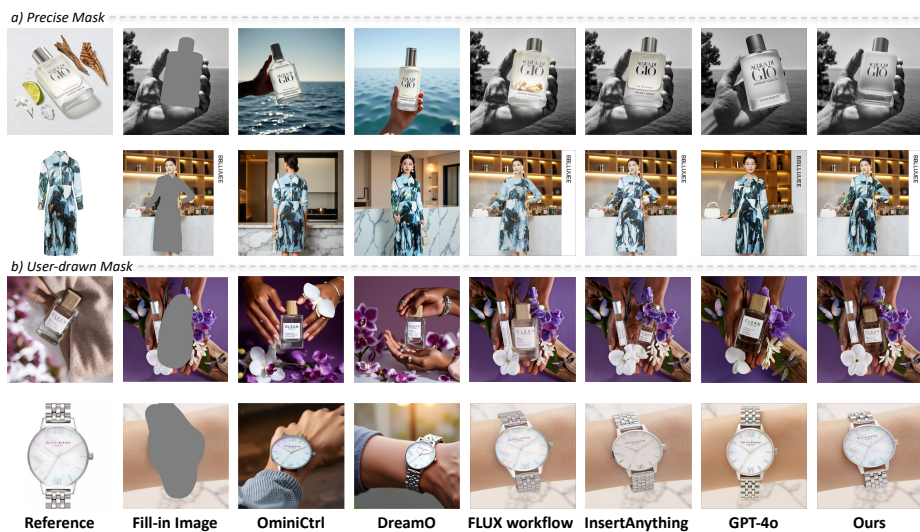


Figure 4: **Qualitative comparison of position-aware customization under precise-mask and user-drawn-mask settings.** OminiCtrl and DreamO lack support for fill-in inputs. *IC-Custom* achieves high-quality customization with harmonious lighting, shadows, and perspectives.

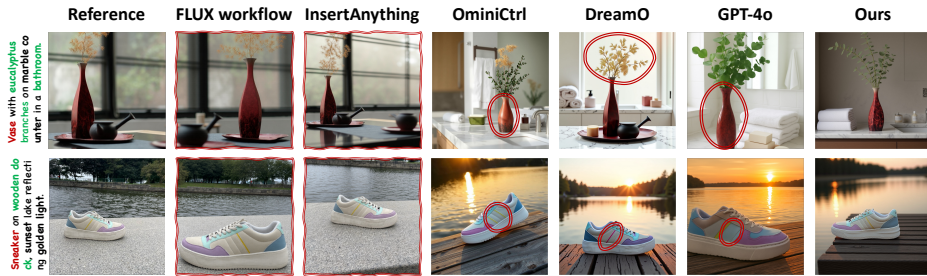


Figure 5: **Qualitative comparison on position-free customization.** *IC-Custom* achieves more realistic, coherent, and detailed customization. Red circles highlight incorrect regions or details.

aware customization, whereas OminiCtrl and DreamO target position-free customization. Beyond evaluating each method in its native setting, we also adapt the other baselines to complementary scenarios—feeding blank fill-in images to FLUX.1 workflow and Insert Anything to approximate position-free customization, and prompting OminiCtrl and DreamO with text descriptions of the identity embedded in the fill-in image scene to approximate position-aware customization. GPT-4o, in contrast, is a unified vision–language system. We therefore provide it with alternating image–text pairs and explicit instructions to perform each customization mode. For completeness, and despite space constraints, we also include an evaluation of ACE++ in Appendix Sec. C.

4.2 POSITION-AWARE CUSTOMIZATION

Quantitative Comparisons. Tab. 2 reports quantitative results on *ProductBench* using both precise and user-drawn masks. *IC-Custom* achieves state-of-the-art identity consistency and text alignment, particularly under the more practical user-drawn mask setting (e.g., DINO-I 63.28 vs. 62.26). Although the adapted OminiCtrl, DreamO, and GPT-4o achieve reasonable scores, they essentially regenerate images rather than perform reference-based image filling (see the following paragraph). Despite being specifically designed for position-aware customization, FLUX.1 workflow and Insert Anything still underperform compared with our method.

Qualitative Comparisons. Fig. 4 presents qualitative comparisons on *ProductBench*. OminiCtrl, DreamO, and GPT-4o tend to regenerate entire images rather than perform position-aware cus-

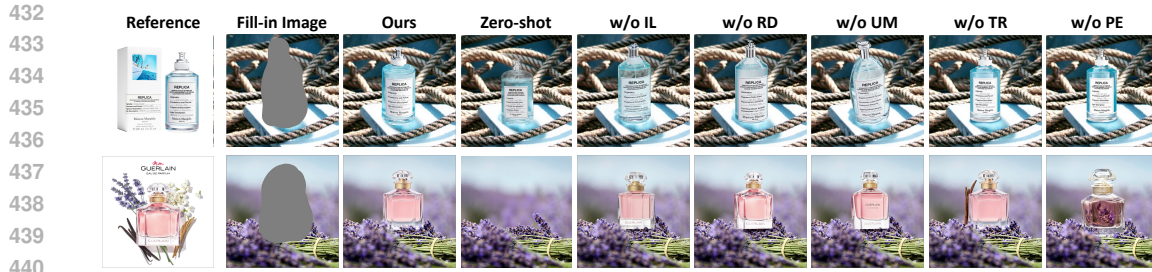


Figure 6: **Ablation Visualization.** Qualitative results show that our model preserves identity consistency while enabling harmonious customization. Abbreviations are as follows: Zero-shot = zero-shot inference without fine-tuning; w/o IL = without training Input Layers; w/o RD = without using Real Data for training; w/o UM = without using User-drawn Mask for training; w/o TR = without Task-oriented Register tokens; w/o PE = without Boundary-aware Positional Embeddings.

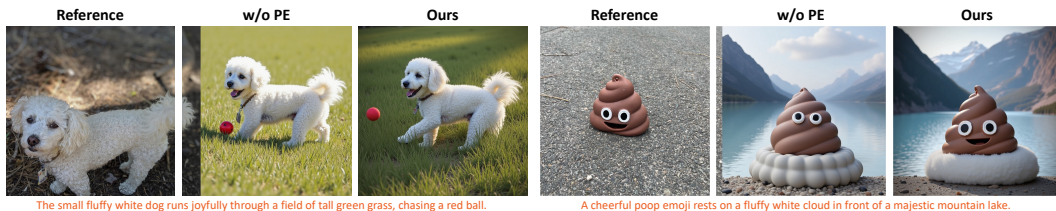


Figure 7: **Effect of Boundary-aware Positional Embeddings.** Without Boundary-aware Positional Embeddings (PE), position-free customization can produce blurred or ambiguous boundaries between the reference and generated content. Incorporating these embeddings sharpens boundaries.

tomization, for example in the precise-mask try-on case (second row) where the human’s face is completely altered. FLUX.1 workflow and Insert Anything also produce noticeable artifacts and weaker identity preservation compared with our model. Moreover, under the user-drawn mask setting, our method generates content with harmonious size, shape, and appearance instead of merely filling the mask region. Thanks to its unified in-context formulation, *IC-Custom* delivers position-aware customization with harmonious lighting, shadows, textures, and materials. More visual results are provided in Appendix Sec. H.

4.3 POSITION-FREE CUSTOMIZATION

Quantitative Comparisons. FLUX.1 workflow and Insert Anything lack position-free customization capability and, even after adaptation, merely replicate the reference (see the following paragraph), so we exclude them. As shown in the DreamBench section of Tab. 2, OminiCtrl shows poor identity consistency (low DINO-I and CLIP-I), while DreamO and GPT-4o, though strong, still lag behind our approach. Trained on a high-quality mix of real and synthetic data with a unified customization representation, our method achieves state-of-the-art performance across all metrics.

Qualitative Comparisons. Figure 5 presents qualitative comparisons in the position-free setting. FLUX.1 workflow and Insert Anything fail to achieve true position-free customization, tending instead to replicate the reference identity image. OminiCtrl and DreamO produce results that are less realistic and less coherent than ours, while GPT-4o, despite strong instruction-following capabilities, sometimes loses fine-grained identity details. In contrast, *IC-Custom* consistently generates diverse, harmonious, and identity-consistent results. More visual results are provided in Appendix Sec. H.

4.4 HUMAN EVALUATION

We conducted a user study with 20 participants on 50 randomly selected samples from both position-aware and position-free subsets. For each sample, participants were asked to identify the best-performing model across three dimensions: identity consistency, harmony, and text alignment. As

486 shown in Tab. 3(a), our method receives the highest human preference across all three dimensions
 487 compared with existing approaches. As FLUX.1 workflow and Insert Anything only take images as
 488 input, we exclude them from the rating of text alignment.
 489

490 4.5 ABLATION STUDIES 491

492 We present ablation studies of *IC-Custom* in Tab. 3(b), examining model architecture, training data
 493 sources, and training strategies. We first establish zero-shot performance as a baseline. We then
 494 validate several key design choices: ① Without training the DiT image and text input layers (w/o
 495 IL), the model struggles to transfer the pre-trained diffusion prior to customization tasks, especially
 496 under user-drawn mask settings; ② Training solely on synthetic data (w/o RD) weakens identity
 497 consistency and realism; ③ Omitting user-drawn mask data during training (w/o UM) substantially
 498 reduces performance on free-form masks; ④ Removing Task-oriented Register tokens (w/o TR) or
 499 Boundary-aware Positional Embeddings (w/o PE) also degrades performance.

500 Qualitative results in Fig. 6 confirm these findings: all ablated variants introduce artifacts or shape
 501 distortions, whereas our full model preserves identity while naturally integrating it into the scene,
 502 yielding harmonious lighting and perspective. While the ablation variants exhibit different imper-
 503fections, a representative case is w/o TR: Fig. 6 (second row) shows unwanted structures form-
 504ing around the imprecise user-drawn mask boundaries, where background completion is expected.
 505 Adding TR helps alleviate this by enhancing the model’s ability to distinguish and adapt to different
 506 task types. We also observe that, in position-free customization, performing flow matching on both
 507 the reference and output images tends to blur their boundaries—an issue alleviated by incorporating
 508 Boundary-aware Positional Embeddings (see Fig. 7).

509 In addition, since the position-aware setting allows multiple input-conditioning configurations to be
 510 integrated, we conduct further ablations in Appendix Sec. B to evaluating performance under these
 511 settings. *IC-Custom* remains robust and reliable across all input-conditioning modes.

513 5 CONCLUSIONS AND LIMITATIONS

515 This paper presents *IC-Custom*, a flexible and effective framework for image customization. Our
 516 approach introduces four key contributions: (1) an in-context customization paradigm that unifies
 517 position-free and position-aware image customization; (2) a novel In-Context Multi-Modal Atten-
 518 tion (ICMA) mechanism to adapt to different customization settings; (3) a high-quality identity-
 519 consistent dataset sourced primarily from real-world images; and (4) an evaluation benchmark with
 520 a balanced distribution of rigid and non-rigid customization tasks. Extensive experiments demon-
 521 strate that *IC-Custom* achieves state-of-the-art performance across multiple metrics.

522 Despite these achievements, our method does not explicitly model viewpoint, lighting, geometry,
 523 or other 3D scene properties, which we plan to address in future work. We also provide an initial
 524 exploration of multi-reference customization in Appendix F. In addition, Appendix E presents a
 525 preliminary study on geometric consistency, Appendix G illustrates the cross-domain customization
 526 capability of our model, and Appendix D demonstrates its multi-round iterative customization per-
 527 formance. We also include representative failure cases and corresponding analyses in Appendix I.

529 REFERENCES

531 Omri Avrahami, Kfir Aberman, Ohad Fried, Daniel Cohen-Or, and Dani Lischinski. Break-a-scene:
 532 Extracting multiple concepts from a single image. In *SIGGRAPH Asia 2023 Conference Papers*,
 533 pp. 1–12, 2023.

534 Shuai Bai, Keqin Chen, Xuejing Liu, Jialin Wang, Wenbin Ge, Sibo Song, Kai Dang, Peng Wang,
 535 Shijie Wang, Jun Tang, et al. Qwen2. 5-vl technical report. *arXiv preprint arXiv:2502.13923*,
 536 2025.

538 Xi Chen, Yutong Feng, Mengting Chen, Yiyang Wang, Shilong Zhang, Yu Liu, Yujun Shen, and
 539 Hengshuang Zhao. Zero-shot image editing with reference imitation. *Advances in Neural Infor-
 mation Processing Systems*, 37:84010–84032, 2024a.

540 Xi Chen, Lianghua Huang, Yu Liu, Yujun Shen, Deli Zhao, and Hengshuang Zhao. Anydoor: Zero-
 541 shot object-level image customization. In *Proceedings of the IEEE/CVF conference on computer*
 542 *vision and pattern recognition*, pp. 6593–6602, 2024b.

543 Xi Chen, Zhifei Zhang, He Zhang, Yuqian Zhou, Soo Ye Kim, Qing Liu, Yijun Li, Jianming Zhang,
 544 Nanxuan Zhao, Yilin Wang, et al. Unireal: Universal image generation and editing via learning
 545 real-world dynamics. *arXiv preprint arXiv:2412.07774*, 2024c.

546 Prafulla Dhariwal and Alexander Nichol. Diffusion models beat gans on image synthesis. *Advances*
 547 *in neural information processing systems*, 34:8780–8794, 2021.

548 Patrick Esser, Sumith Kulal, Andreas Blattmann, Rahim Entezari, Jonas Müller, Harry Saini, Yam
 549 Levi, Dominik Lorenz, Axel Sauer, Frederic Boesel, et al. Scaling rectified flow transformers
 550 for high-resolution image synthesis. In *Forty-first international conference on machine learning*,
 551 2024a.

552 Patrick Esser, Sumith Kulal, Andreas Blattmann, Rahim Entezari, Jonas Müller, Harry Saini, Yam
 553 Levi, Dominik Lorenz, Axel Sauer, Frederic Boesel, et al. Scaling rectified flow transformers
 554 for high-resolution image synthesis. In *Forty-first international conference on machine learning*,
 555 2024b.

556 Rinon Gal, Yuval Alaluf, Yuval Atzmon, Or Patashnik, Amit H Bermano, Gal Chechik, and Daniel
 557 Cohen-Or. An image is worth one word: Personalizing text-to-image generation using textual
 558 inversion. *arXiv preprint arXiv:2208.01618*, 2022.

559 Ian Goodfellow, Jean Pouget-Abadie, Mehdi Mirza, Bing Xu, David Warde-Farley, Sherjil Ozair,
 560 Aaron Courville, and Yoshua Bengio. Generative adversarial networks. *Communications of the*
 561 *ACM*, 63(11):139–144, 2020.

562 Hailong Guo, Bohan Zeng, Yiren Song, Wentao Zhang, Chuang Zhang, and Jiaming Liu.
 563 Any2anytryon: Leveraging adaptive position embeddings for versatile virtual clothing tasks.
 564 *arXiv preprint arXiv:2501.15891*, 2025.

565 Jonathan Ho, Ajay Jain, and Pieter Abbeel. Denoising diffusion probabilistic models. *Advances in*
 566 *neural information processing systems*, 33:6840–6851, 2020.

567 Edward J Hu, Yelong Shen, Phillip Wallis, Zeyuan Allen-Zhu, Yuanzhi Li, Shean Wang, Lu Wang,
 568 Weizhu Chen, et al. Lora: Low-rank adaptation of large language models. *ICLR*, 1(2):3, 2022.

569 Aaron Hurst, Adam Lerer, Adam P Goucher, Adam Perelman, Aditya Ramesh, Aidan Clark, AJ Os-
 570 trow, Akila Welihinda, Alan Hayes, Alec Radford, et al. Gpt-4o system card. *arXiv preprint*
 571 *arXiv:2410.21276*, 2024a.

572 Aaron Hurst, Adam Lerer, Adam P Goucher, Adam Perelman, Aditya Ramesh, Aidan Clark, AJ Os-
 573 trow, Akila Welihinda, Alan Hayes, Alec Radford, et al. Gpt-4o system card. *arXiv preprint*
 574 *arXiv:2410.21276*, 2024b.

575 Diederik P Kingma, Max Welling, et al. Auto-encoding variational bayes, 2013a.

576 Diederik P Kingma, Max Welling, et al. Auto-encoding variational bayes, 2013b.

577 Alexander Kirillov, Eric Mintun, Nikhila Ravi, Hanzi Mao, Chloe Rolland, Laura Gustafson, Tete
 578 Xiao, Spencer Whitehead, Alexander C Berg, Wan-Yen Lo, et al. Segment anything. In *Proceed-
 579 ings of the IEEE/CVF International Conference on Computer Vision (ICCV)*, October 2023.

580 Nupur Kumari, Xi Yin, Jun-Yan Zhu, Ishan Misra, and Samaneh Azadi. Generating multi-image
 581 synthetic data for text-to-image customization. *arXiv preprint arXiv:2502.01720*, 2025.

582 Black Forest Labs. Flux. <https://github.com/black-forest-labs/flux>, 2024a.

583 Black Forest Labs. Flux.1-fill-dev. <https://huggingface.co/black-forest-labs/FLUX.1-Fill-dev>, 2024b.

584 Black Forest Labs. Flux.1-redux-dev. <https://huggingface.co/black-forest-labs/FLUX.1-Redux-dev/>, 2024c.

594 Black Forest Labs, Stephen Batifol, Andreas Blattmann, Frederic Boesel, Saksham Consul, Cyril
 595 Diagne, Tim Dockhorn, Jack English, Zion English, Patrick Esser, et al. Flux. 1 kontext:
 596 Flow matching for in-context image generation and editing in latent space. *arXiv preprint*
 597 *arXiv:2506.15742*, 2025.

598 Zhong-Yu Li, Ruoyi Du, Juncheng Yan, Le Zhuo, Zhen Li, Peng Gao, Zhanyu Ma, and Ming-Ming
 599 Cheng. Visualcloze: A universal image generation framework via visual in-context learning.
 600 *arXiv preprint arXiv:2504.07960*, 2025.

601 Yaron Lipman, Ricky TQ Chen, Heli Ben-Hamu, Maximilian Nickel, and Matt Le. Flow matching
 602 for generative modeling. In *11th International Conference on Learning Representations, ICLR*
 603 2023, 2023.

604 Xingchao Liu, Chengyue Gong, and Qiang Liu. Flow straight and fast: Learning to generate and
 605 transfer data with rectified flow. *arXiv preprint arXiv:2209.03003*, 2022.

606 Ilya Loshchilov and Frank Hutter. Decoupled weight decay regularization. *arXiv preprint*
 607 *arXiv:1711.05101*, 2017.

608 Chaojie Mao, Jingfeng Zhang, Yulin Pan, Zeyinzi Jiang, Zhen Han, Yu Liu, and Jingren Zhou.
 609 Ace++: Instruction-based image creation and editing via context-aware content filling. *arXiv*
 610 *preprint arXiv:2501.02487*, 2025.

611 Chong Mou, Yanze Wu, Wenxu Wu, Zinan Guo, Pengze Zhang, Yufeng Cheng, Yiming Luo, Fei
 612 Ding, Shiwen Zhang, Xinghui Li, et al. Dreamo: A unified framework for image customization.
 613 *arXiv preprint arXiv:2504.16915*, 2025.

614 Alex Nichol, Prafulla Dhariwal, Aditya Ramesh, Pranav Shyam, Pamela Mishkin, Bob McGrew,
 615 Ilya Sutskever, and Mark Chen. Glide: Towards photorealistic image generation and editing with
 616 text-guided diffusion models. *arXiv preprint arXiv:2112.10741*, 2021.

617 Maxime Oquab, Timothée Darcet, Théo Moutakanni, Huy Vo, Marc Szafraniec, Vasil Khalidov,
 618 Pierre Fernandez, Daniel Haziza, Francisco Massa, Alaaeldin El-Nouby, et al. Dinov2: Learning
 619 robust visual features without supervision. *arXiv preprint arXiv:2304.07193*, 2023.

620 William Peebles and Saining Xie. Scalable diffusion models with transformers. In *Proceedings of*
 621 *the IEEE/CVF international conference on computer vision*, pp. 4195–4205, 2023a.

622 William Peebles and Saining Xie. Scalable diffusion models with transformers. In *Proceedings of*
 623 *the IEEE/CVF international conference on computer vision*, pp. 4195–4205, 2023b.

624 Alec Radford, Jong Wook Kim, Chris Hallacy, Aditya Ramesh, Gabriel Goh, Sandhini Agarwal,
 625 Girish Sastry, Amanda Askell, Pamela Mishkin, Jack Clark, et al. Learning transferable visual
 626 models from natural language supervision. In *International conference on machine learning*, pp.
 627 8748–8763, 2021.

628 Colin Raffel, Noam Shazeer, Adam Roberts, Katherine Lee, Sharan Narang, Michael Matena, Yanqi
 629 Zhou, Wei Li, and Peter J Liu. Exploring the limits of transfer learning with a unified text-to-text
 630 transformer. *Journal of machine learning research*, 21(140):1–67, 2020.

631 Aditya Ramesh, Prafulla Dhariwal, Alex Nichol, Casey Chu, and Mark Chen. Hierarchical text-
 632 conditional image generation with clip latents. *arXiv preprint arXiv:2204.06125*, 1(2):3, 2022.

633 Tianhe Ren, Shilong Liu, Ailing Zeng, Jing Lin, Kunchang Li, He Cao, Jiayu Chen, Xinyu Huang,
 634 Yukang Chen, Feng Yan, et al. Grounded sam: Assembling open-world models for diverse visual
 635 tasks. *arXiv preprint arXiv:2401.14159*, 2024.

636 Robin Rombach, Andreas Blattmann, Dominik Lorenz, Patrick Esser, and Björn Ommer. High-
 637 resolution image synthesis with latent diffusion models. In *Proceedings of the IEEE/CVF confer-
 638 ence on computer vision and pattern recognition*, pp. 10684–10695, 2022.

639 Olaf Ronneberger, Philipp Fischer, and Thomas Brox. U-net: Convolutional networks for biomed-
 640 ical image segmentation. In *Medical image computing and computer-assisted intervention-
 641 MICCAI 2015: 18th international conference, Munich, Germany, October 5-9, 2015, proceed-
 642 ings, part III 18*, pp. 234–241. Springer, 2015.

648 Nataniel Ruiz, Yuanzhen Li, Varun Jampani, Yael Pritch, Michael Rubinstein, and Kfir Aberman.
 649 Dreambooth: Fine tuning text-to-image diffusion models for subject-driven generation. In *Pro-
 650 ceedings of the IEEE/CVF conference on computer vision and pattern recognition*, pp. 22500–
 651 22510, 2023a.

652 Nataniel Ruiz, Yuanzhen Li, Varun Jampani, Yael Pritch, Michael Rubinstein, and Kfir Aberman.
 653 Dreambooth: Fine tuning text-to-image diffusion models for subject-driven generation. In *Pro-
 654 ceedings of the IEEE/CVF conference on computer vision and pattern recognition*, pp. 22500–
 655 22510, 2023b.

656 Jascha Sohl-Dickstein, Eric Weiss, Niru Maheswaranathan, and Surya Ganguli. Deep unsupervised
 657 learning using nonequilibrium thermodynamics. In *International conference on machine learn-
 658 ing*, pp. 2256–2265. pmlr, 2015.

659 Wensong Song, Hong Jiang, Zongxing Yang, Ruijie Quan, and Yi Yang. Insert anything: Image
 660 insertion via in-context editing in dit. *arXiv preprint arXiv:2504.15009*, 2025.

661 Jianlin Su, Murtadha Ahmed, Yu Lu, Shengfeng Pan, Wen Bo, and Yunfeng Liu. Roformer: En-
 662 hanced transformer with rotary position embedding. *Neurocomputing*, 568:127063, 2024.

663 Zhenxiong Tan, Songhua Liu, Xingyi Yang, Qiaochu Xue, and Xinchao Wang. Ominicontrol: Min-
 664 imal and universal control for diffusion transformer. *arXiv preprint arXiv:2411.15098*, 2024.

665 Gemini Team, Rohan Anil, Sebastian Borgeaud, Jean-Baptiste Alayrac, Jiahui Yu, Radu Soricut,
 666 Johan Schalkwyk, Andrew M Dai, Anja Hauth, Katie Millican, et al. Gemini: a family of highly
 667 capable multimodal models. *arXiv preprint arXiv:2312.11805*, 2023.

668 Yoad Tewel, Omri Kaduri, Rinon Gal, Yoni Kasten, Lior Wolf, Gal Chechik, and Yuval Atzmon.
 669 Training-free consistent text-to-image generation. *ACM Transactions on Graphics (TOG)*, 43(4):
 670 1–18, 2024.

671 Ashish Vaswani, Noam Shazeer, Niki Parmar, Jakob Uszkoreit, Llion Jones, Aidan N Gomez,
 672 Łukasz Kaiser, and Illia Polosukhin. Attention is all you need. *Advances in neural informa-
 673 tion processing systems*, 30, 2017.

674 Jianyuan Wang, Minghao Chen, Nikita Karaev, Andrea Vedaldi, Christian Rupprecht, and David
 675 Novotny. Vggt: Visual geometry grounded transformer. In *Proceedings of the Computer Vision
 676 and Pattern Recognition Conference*, pp. 5294–5306, 2025.

677 Rui Wang, Hailong Guo, Jiaming Liu, Huaxia Li, Haibo Zhao, Xu Tang, Yao Hu, Hao Tang,
 678 and Peipei Li. Stablegarment: Garment-centric generation via stable diffusion. *arXiv preprint
 679 arXiv:2403.10783*, 2024.

680 Shaojin Wu, Mengqi Huang, Wenxu Wu, Yufeng Cheng, Fei Ding, and Qian He. Less-to-
 681 more generalization: Unlocking more controllability by in-context generation. *arXiv preprint
 682 arXiv:2504.02160*, 2025.

683 Yuhao Xu, Tao Gu, Weifeng Chen, and Arlene Chen. Ootdiffusion: Outfitting fusion based latent
 684 diffusion for controllable virtual try-on. In *Proceedings of the AAAI Conference on Artificial
 685 Intelligence*, volume 39, pp. 8996–9004, 2025.

686 Hu Ye, Jun Zhang, Sibo Liu, Xiao Han, and Wei Yang. Ip-adapter: Text compatible image prompt
 687 adapter for text-to-image diffusion models. *arXiv preprint arXiv:2308.06721*, 2023a.

688 Hu Ye, Jun Zhang, Sibo Liu, Xiao Han, and Wei Yang. Ip-adapter: Text compatible image prompt
 689 adapter for text-to-image diffusion models. *arXiv preprint arXiv:2308.06721*, 2023b.

690

691

692

693

694

695

696

697

698

699

700

701

702 Appendix

703

704 CONTENTS

705

708	A Related Work	15
709	A.1 Image Diffusion Models	15
710	A.2 Image Customization	15
711		
712	B Ablation on Distinct Input Conditioning Modes	15
713		
714	C Comparison with ACE++	15
715		
716	D Multi-Round Iterative Customization	16
717		
718	E Geometric Consistency Assessment via 3D Reconstruction	17
719		
720	F Preliminary Study on Multi-Reference Customization	17
721		
722	G Cross-Domain Customization Capability	18
723		
724	H Additional Visualization Results	19
725		
726	I Failure Cases	19
727		
728	J Automated Captioning for Data	20
729		
730	K Automated Captioning for Benchmark	20
731		
732	L Training Strategy: Mask Sampling and Augmentation	21
733		
734	M Web Application	21
735		
736	N Ethics Statement	22
737		
738	O Reproducibility Statement	22
739		
740	P LLM Usage Statement	22
741		
742		
743		
744		
745		
746		
747		
748		
749		
750		
751		
752		
753		
754		
755		

756 A RELATED WORK
757758 A.1 IMAGE DIFFUSION MODELS
759

760 Recent advances in diffusion models (Sohl-Dickstein et al., 2015; Ho et al., 2020) have set new
761 benchmarks in image synthesis, outperforming traditional generative models such as Variational
762 Autoencoders (VAE) (Kingma et al., 2013a) and Generative Adversarial Networks (GANs) (Good-
763 fellow et al., 2020) by a significant margin. Consequently, many state-of-the-art text-to-image meth-
764 ods (Dhariwal & Nichol, 2021; Ho et al., 2020; Nichol et al., 2021; Ramesh et al., 2022) have
765 adopted diffusion models as their core generation framework. Early approaches employed a U-
766 Net (Ronneberger et al., 2015) architecture with cross-attention for text-to-image generation, achiev-
767 ing competitive performance and efficiency. Notably, the open-sourcing of Stable Diffusion (Rom-
768 bach et al., 2022) has been a major catalyst for the growth of image synthesis research. More
769 recently, diffusion transformer models, such as SD3 (Esser et al., 2024b) and FLUX (Labs, 2024a),
770 have further advanced the field by integrating transformer architectures (Vaswani et al., 2017) with
771 diffusion models, yielding even higher performance. These models have since been widely applied
772 in various downstream tasks, including depth estimation, image editing, and others.

773 A.2 IMAGE CUSTOMIZATION
774

775 Image customization is typically accomplished by integrating additional control signals from refer-
776 ence images into text-to-image foundation models. One line of work (Wu et al., 2025; Li et al., 2025;
777 Hurst et al., 2024a; Mou et al., 2025; Tan et al., 2024; Chen et al., 2024c) focuses on position-free
778 customization, directly generating identity-consistent images based on input reference images and
779 text, as seen in GPT-4o (Hurst et al., 2024a), DreamO (Mou et al., 2025), and OminiControl (Tan
780 et al., 2024). However, these methods struggle with position-aware customization, particularly when
781 a masked source image is provided, as they cannot preserve the unedited regions. In contrast, meth-
782 ods like Insert Anything (Song et al., 2025) and the FLUX.1-Fill-Redux workflow (Labs, 2024b)
783 specialize in position-aware customization, inserting subjects into masked source images, but lack
784 the capability for position-free customization. Concurrent works such as ACE++ (Mao et al., 2025)
785 and FLUX.1 Kontext (Labs et al., 2025) share similar ideas with our approach, yet differ in innova-
786 tive technical details. In this work, we propose a flexible framework that can address both position-
787 aware customization and position-free customization. We also propose a data curation pipeline to
788 collect high-quality real image data from different product images. Benefiting from this framework
789 and high-quality data, our model achieves highly identity consistent customization, which can be
790 used in real production.

791 B ABLATION ON DISTINCT INPUT CONDITIONING MODES
792

793 In the position-aware customization setting, as illustrated in Fig. 2, our method supports not only
794 the in-context diptych reference but also the integration of both the Redux Encoder and the Text
795 Encoder. To assess how IC-Custom behaves under different combinations of textual and reference-
796 based inputs, we conduct a comprehensive ablation across **four input-conditioning configurations**:
797 ① **Full conditions** (default setting), ② **Redux-only** (no text), ③ **Text-only** (no Redux reference), ④
798 **Diptych-only** (neither text nor Redux; relies solely on the in-context diptych reference). Table 4
799 summarizes the quantitative comparison on ProductBench under both *precise masks* and *user-drawn*
800 *masks*. Across all four input modes, IC-Custom achieves **stable and reliable position-aware per-
801 formance**. Even the diptych-only configuration yields competitive results, indicating that the in-
802 context diptych framework already provides strong customization capability, while the Redux and
803 text inputs act as optional boosters. As shown in Fig. 8, the qualitative comparisons further validate
804 that our method supports all four input-conditioning modes: the full-conditions setting is the most
805 stable overall, yet the reduced-input variants also perform strongly.

806 C COMPARISON WITH ACE++
807

808 ACE++ (Mao et al., 2025) is a concurrent work proposing the Long-context Condition Unit (LCU),
809 conceptually similar to our in-context diptych. However, ACE++ focuses on four separate domain-

Table 4: **Comparison of IC-Custom under four input-conditioning modes in the position-aware setting.** Across all configurations, the model exhibits consistent and robust performance.

Setting	Precise Mask			User-drawn Mask		
	DINO-I \uparrow	CLIP-I \uparrow	CLIP-T \uparrow	DINO-I \uparrow	CLIP-I \uparrow	CLIP-T \uparrow
Full conditions (default)	63.14	81.92	31.75	63.28	81.95	31.80
Redux-only	63.34	81.49	31.37	63.78	81.86	31.10
Text-only	62.96	81.32	31.42	63.04	81.43	31.29
Diptych-only	62.97	81.41	31.41	63.18	81.77	31.30

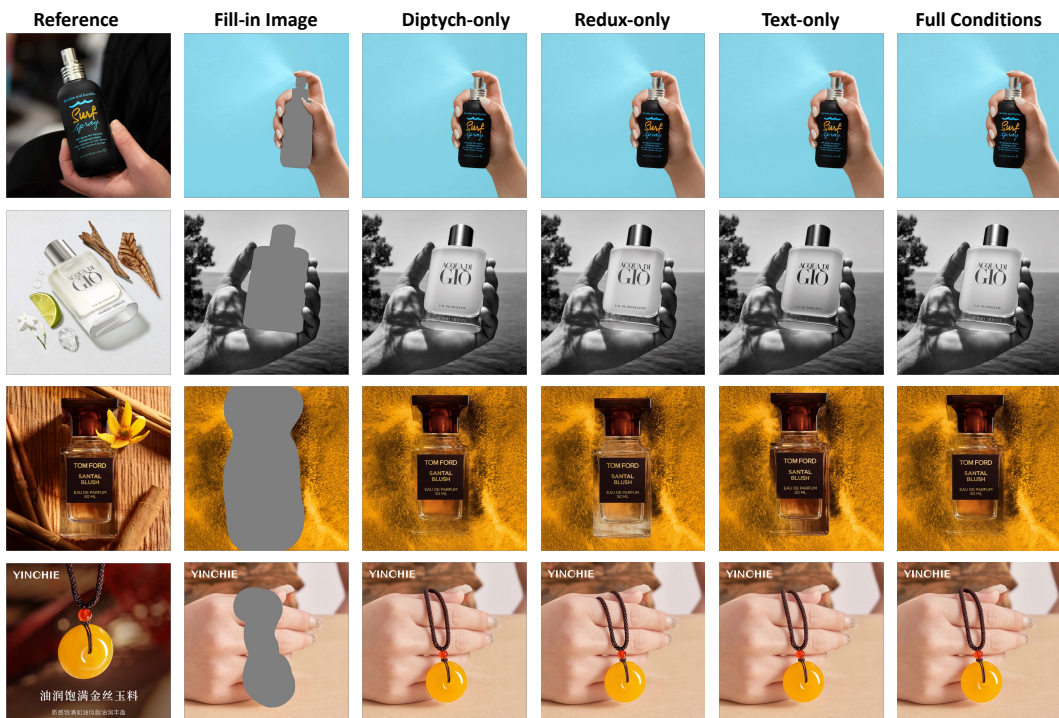


Figure 8: **Qualitative comparison of IC-Custom under four input-conditioning modes in the position-aware setting.** Full conditions yield the most stable results, while the reduced-input modes (Redux-only, text-only, diptych-only) remain strong and coherent.

specific tasks and trains distinct LoRA adapters for each, rather than a unified model handling both position-aware and position-free customization. Moreover, unlike our framework, ACE++ does not incorporate the innovative ICMA module. For a fair comparison on *ProductBench*, we directly use ACE++’s publicly released **subject LoRA adapters** to evaluate its performance under our benchmark. As shown in Tab. 5 and Fig. 9, our model consistently produces more identity-consistent and visually coherent customization results, showing superior perspective, lighting, and shape fidelity while operating as a single unified model rather than multiple task-specific LoRA adapters.

D MULTI-ROUND ITERATIVE CUSTOMIZATION

In the position-aware customization setting, our framework is inherently *composable*, allowing multi-round, iterative refinement of the generated content. As illustrated in Fig. 10, IC-Custom can perform GPT-style, multi-object customization by sequentially applying the model in multiple rounds. We begin by generating an initial customization result based on the in-context diptych reference. This intermediate output can then be reused as a new reference input in subsequent rounds, enabling the model to introduce additional objects or refine fine-grained appearance details step-by-

864 Table 5: **Comparison with ACE++ (Mao et al., 2025) on ProductBench.** Metrics under Precise
 865 Mask (left) and User-drawn Mask (right); higher is better (\uparrow).

Precise Mask				User-drawn Mask			
Method	DINO-I	CLIP-I	CLIP-T	Method	DINO-I	CLIP-I	CLIP-T
ACE++	60.68	81.34	31.64	ACE++	61.26	81.16	31.42
Ours	63.14	81.92	31.75	Ours	63.28	81.95	31.80

a) Precise Mask =  b) User-drawn Mask = 



Reference Fill-in Image ACE++ Ours Reference Fill-in Image ACE++ Ours

866 Figure 9: **Qualitative comparison with ACE++ (Mao et al., 2025).** Our method produces more
 867 identity-consistent and harmonious customization results. We compare our unified framework
 868 with ACE++ on *ProductBench*.

890 step. By iteratively composing these rounds, users can achieve complex, multi-object customization
 891 scenarios while preserving spatial coherence and identity consistency throughout the process.

E GEOMETRIC CONSISTENCY ASSESSMENT VIA 3D RECONSTRUCTION

896 To explicitly validate whether the customized results generated by our method maintain geometric
 897 consistency with the reference identity, we conduct a 3D reconstruction analysis using VGTT (Wang
 898 et al., 2025). Specifically, we feed both the reference and generated images into VGTT to assess
 899 the recoverability of the underlying 3D structure. As illustrated in Figure 11, VGTT effectively
 900 aggregates geometric cues from the generated distinct views, successfully reconstructing 3D point
 901 clouds with faithful shapes. Notably, despite the absence of explicit 3D modeling, these results
 902 indicate that our method not only preserves visual semantics but also achieves robust geometric
 903 alignment with the reference subject. Nevertheless, we acknowledge that our current framework
 904 does not support explicit control over the pose of the customized results. Such precise viewpoint
 905 controllability pertains to the domain of generative rendering, which lies outside the scope of this
 906 paper and is reserved for future work.

F PRELIMINARY STUDY ON MULTI-REFERENCE CUSTOMIZATION

907 Benefiting from the learnable task-oriented register tokens and boundary-aware positional embed-
 908 dings introduced in our **In-Context Multi-Modal Attention (ICMA)**, our model can accurately
 909 distinguish customization types and the boundaries between inputs and outputs. This naturally ex-
 910 tends to **multi-reference customization**, where multiple reference images of the same identity (but
 911 from different scenes) are provided—not as multi-image fusion, but as separate context cues. By
 912 aggregating information from multiple references, our model better preserves identity fidelity and
 913 fine details. To support this setting, we concatenate multiple reference images with the fill-in noise
 914 input and introduce an additional **index embedding** in the boundary-aware positional embeddings
 915 to differentiate reference indices. Formally, we extend the diptych structure to polyptych, modi-
 916 fying Eq. 5 to $X_0 = [C_1; C_{I_1}, C_{I_2}, \dots, C_{I_n}]$. Additionally, to distinguish different references, we

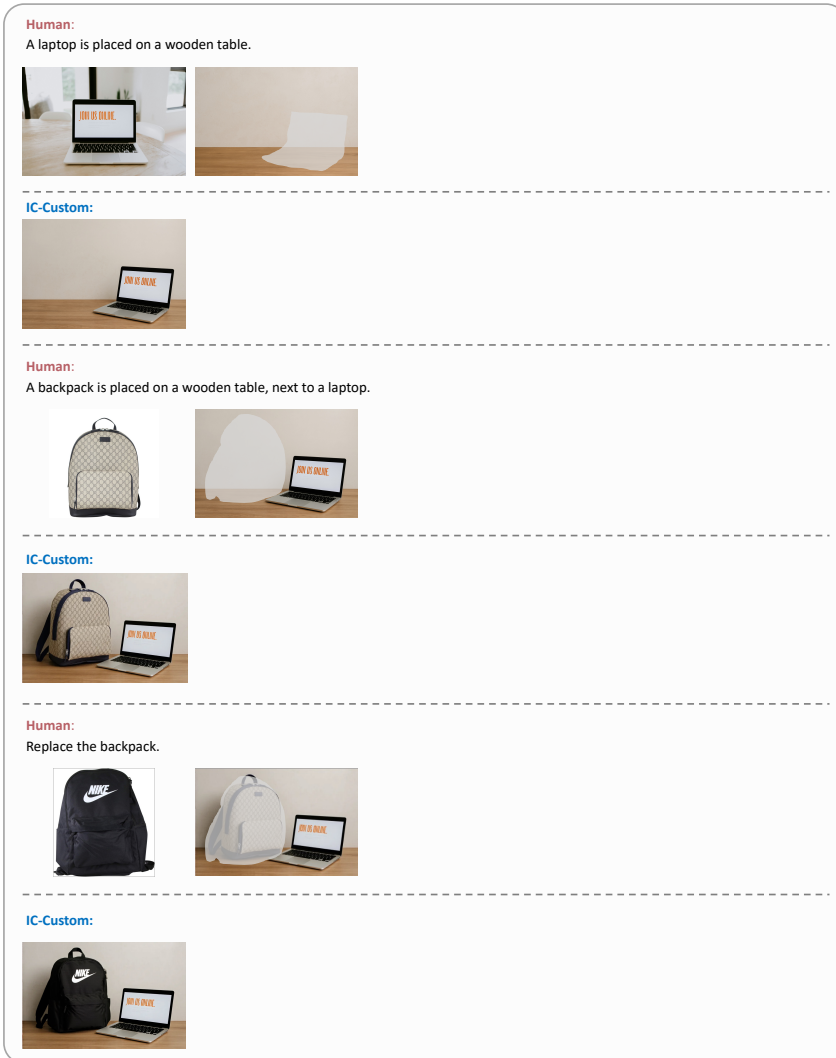


Figure 10: Illustration of multi-round iterative customization: add laptop → add backpack → replace backpack, demonstrating IC-Custom’s extended application for multi-object customization.

draw inspiration from DreamO (Mou et al., 2025) by introducing learnable Index embeddings. The key difference is that we add these embeddings in the ICMA module rather than the input tokens. Specifically, we extend the function $\mathcal{P}(x)$ in Eq. 6 as $\mathcal{P}(x) = x + [\mathcal{E}_R + \mathcal{E}_I; \mathcal{E}_F] + \mathcal{R}(x)$, where $\mathcal{E}_I \in \mathbb{R}^{k, m/k \times d}$ are the learnable Index embeddings, $\mathcal{E}_R \in \mathbb{R}^{m \times d}$ and $\mathcal{E}_F \in \mathbb{R}^{n \times d}$ are the learnable Reference and Fill embeddings. We also curated a multi-reference dataset containing **2K real-world** and **2K synthetic polyptychs** for training. In Fig. 12, our multi-reference approach aggregates information from multiple references (e.g., different viewpoints) to better preserve object identity details and textures. This preliminary exploration highlights the broader capability and scalability of our unified customization model, and we plan to further explore this direction in future work.

G CROSS-DOMAIN CUSTOMIZATION CAPABILITY

To further validate the Cross-Domain Customization Capability of our method, we conducted experiments on position-aware customization tasks across multiple domains, including cross-style, cross-pose, and cross-object scenarios. Fig. 13 highlight the robustness and flexibility of our method in handling a wide range of cross-domain customization tasks. However, we clarify that explicit style-

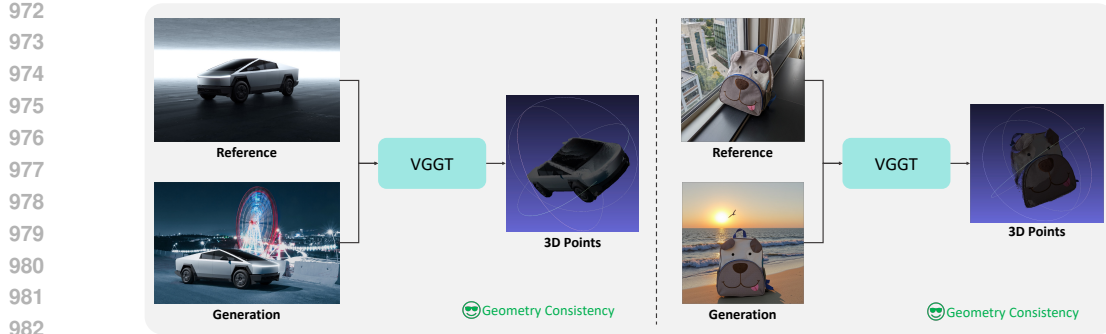


Figure 11: **Evaluation of Geometric Consistency.** Visual comparison of 3D reconstructions derived from reference and generated images.

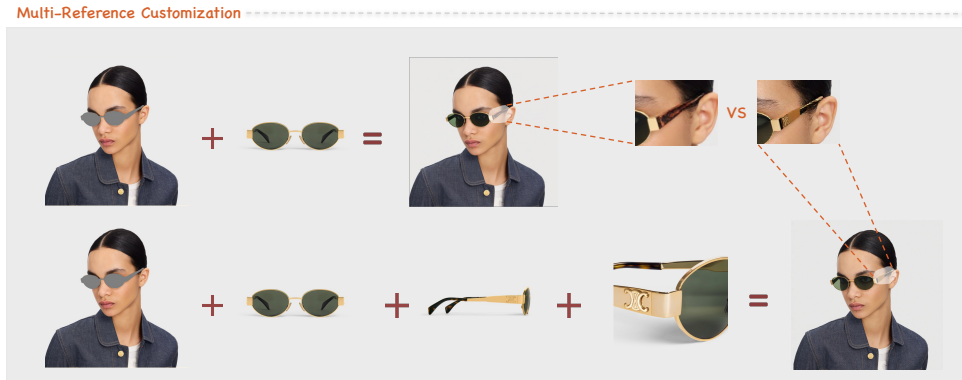


Figure 12: **Multi-Reference Customization.** By aggregating multiple reference images of the same identity from different environments and viewpoints, our model preserves richer details and textures. For example, when a single reference view omits the glasses’ temples, the model must hallucinate them; with multiple viewpoints including the temples, it reconstructs the object more completely.

content disentanglement is not a primary objective of our work. As such, it is challenging to specify a reference style image as input to achieve more specific style-driven customization.

H ADDITIONAL VISUALIZATION RESULTS

Figure 17 shows additional position-free customization results, where our model seamlessly generates novel scenes that preserve the reference identity based on text descriptions. Figure 18 presents additional position-aware customization results, demonstrating its ability to accurately insert or edit images with different materials and textures while maintaining identity consistency.

I FAILURE CASES

While our method demonstrates robust performance across diverse scenarios, we acknowledge specific limitations. We present several failure cases where the performance of the model degrades under certain conditions.

As illustrated in Fig. 14, in **position-aware customization**, challenges arise when the user-provided mask is **ambiguous, extremely incomplete, or excessively small**. For instance, in the first row of Fig. 14, an ambiguous or incomplete mask leads to the generation of erroneous content instead of the intended duckling; however, dilating the mask into a rectangular bounding box significantly improves performance. Furthermore, as shown in the second column of the second row, when the mask is excessively small, the model fails to inject the target subject entirely due to insufficient position guidance.



Figure 13: **Qualitative results of cross-domain customization.** Demonstrating the effectiveness of our method in handling cross-style, cross-pose, and cross-object customization tasks.

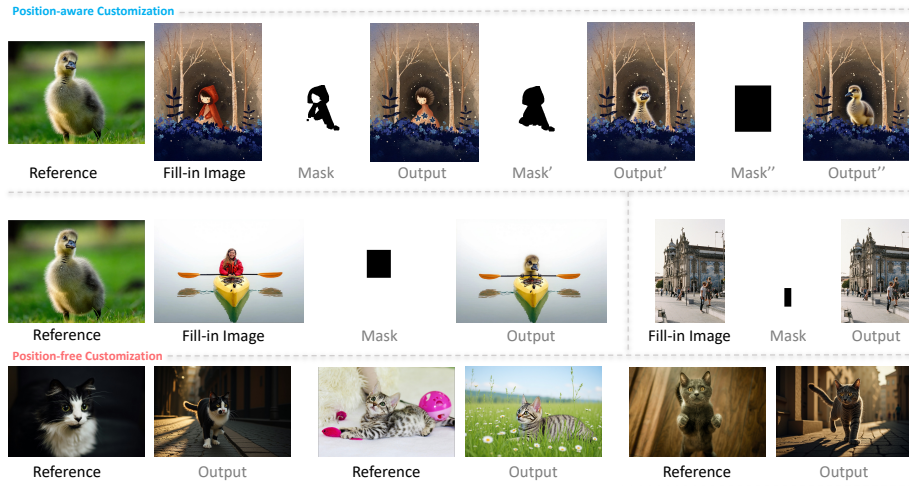


Figure 14: **Failure cases.** We present several failure cases that highlight the limitations of our method and suggest areas for potential improvement.

In **position-free customization**, the model’s performance is hindered when the reference identity lacks **essential details** or features **complex textures**. For example, in the position-free customization row of Fig. 14, the texture patterns of the generated cat are not perfectly consistent with the reference image, indicating a difficulty in faithfully reconstructing high-frequency details for complex subjects. We aim to further investigate these boundary conditions and enhance the robustness of our framework in future work.

J AUTOMATED CAPTIONING FOR DATA

We use Qwen-VL2.5 (Bai et al., 2025) to automatically generate text annotations for our data. Specifically, each concatenated pair of identity-consistent images is fed into Qwen-VL2.5 with custom-designed instructions to generate captions, as illustrated in Fig. 15.

K AUTOMATED CAPTIONING FOR BENCHMARK

Our benchmark consists of two parts: *ProductBench* for evaluating position-aware customization and DreamBench (Ruiz et al., 2023a) for evaluating position-free customization. For *ProductBench*, we apply the captioning approach described in Sec. J to generate input captions. For DreamBench,

1080
1081
1082
1083
1084
1085

Human:

I've shown you 2 images that contains the same object. Create a short description of this 2-scene image. Each scene detail should be marked with [SCENE-1], [SCENE-2] indicating the start of each scene's description. Don't use phrases like 'the first image' or 'the second image' as the images are unordered - describe each independently without referencing their order. Focus on describing the key visual contents, effects, colors, textures and styling details of each object. The descriptions for [SCENE-1], [SCENE-2] should be completely independent and should not reference each other. The description should not exceed 512 words. Please strictly follow this format without any additional content.

**VLM (Qwen-VL):**

[SCENE-1] The Murad Clarifying Toner bottle is set against a neutral beige background. The bottle is upright, and the label faces forward, clearly displaying the product information. The golden capsules are scattered around the bottle, adding a touch of contrast to the warm-toned background. The lighting is soft and even, highlighting the transparency of the bottle and the vibrant blue of the label.

[SCENE-2] The Murad Clarifying Toner bottle is placed on a light blue background, creating a cool-toned setting. The bottle is also upright, and the label is visible, showing the product name and description. The background features a subtle pattern of water droplets, enhancing the fresh and hydrating theme associated with the toner. The overall ambiance is serene and refreshing, complementing the product's purpose.

1100
1101
1102
1103
1104

Figure 15: **Example of automated text prompt annotation.** A concatenated pair of identity-consistent images is fed into Qwen-VL2.5 (Bai et al., 2025) with custom-designed instructions to generate corresponding captions for our data.

1105
1106
1107
1108
1109

which targets position-free customization, we provide the reference image together with prompts designed to elicit creative yet identity-consistent outputs; an example of this prompting strategy is shown in Fig. 16.

1110
1111

L TRAINING STRATEGY: MASK SAMPLING AND AUGMENTATION

1112
1113
1114
1115
1116
1117
1118
1119

To enhance model flexibility and robustness, we randomly sample mask types during training: position-aware masks with a probability of 0.6 and position-free masks with 0.4. Within the position-aware cases, we further draw user-drawn masks with 0.75 probability and precise masks with 0.25, assigning higher probabilities to harder tasks to provide more training iterations. In addition, we convert precise masks from Grounded SAM into user-drawn masks via standard image-morphology operations such as dilation, erosion, opening, and closing.

1120
1121

M WEB APPLICATION

1122
1123
1124
1125
1126
1127
1128
1129
1130
1131
1132
1133

We implement a web application using Hugging Face Gradio² to provide a simple and seamless interface for both position-free and position-aware customization (see Fig. 19 and Fig. 20). Users first select a customization mode and upload a reference image. In the **position-aware mode**, they choose a mask type (precise or user-drawn), upload the fill-in image, optionally refine the mask (via SAM for precise masks or manual brushing for user-drawn masks), and provide an optional text prompt before running the model. In the **position-free mode**, users directly supply a text prompt describing the desired scene or use the built-in VLM-based prompt auto-generation tool prior to execution. This web application provides a simple, unified interface for both position-aware and position-free customization, enabling users to interactively explore our model's capabilities with minimal setup. We will release the full code and the web application as open source to support reproducibility and community adoption.

²<https://www.gradio.app/>

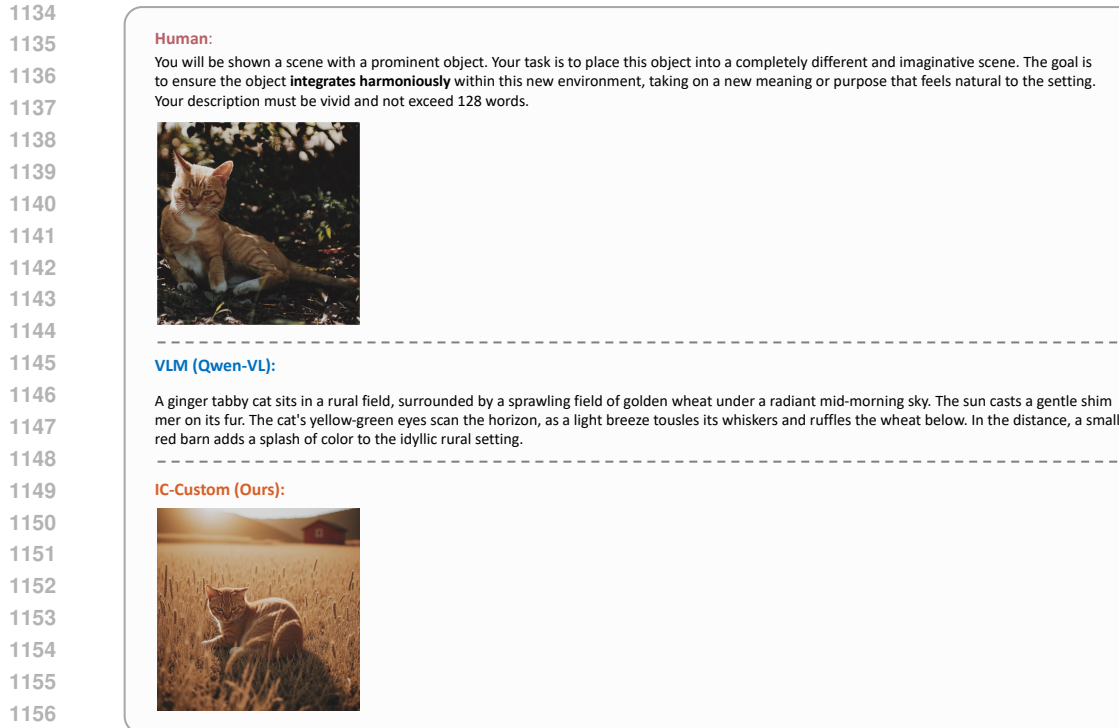


Figure 16: **Example of DreamBench captioning and generated output.** We illustrate our prompting process for DreamBench, where a reference image and custom instructions are provided to a vision–language model to generate creative, identity-consistent captions. The figure also shows an example image generated by our method using the curated reference and caption.

N ETHICS STATEMENT

This work complies with the ICLR Code of Ethics.³ Our study does not involve human or animal subjects, personally identifiable information, or sensitive demographic attributes. All datasets are either publicly available or internally curated, and will be verified for proper licensing prior to open-sourcing. We also adopt the SafeChecker from the Diffusers FLUX.1 framework to filter potentially harmful outputs (e.g., sexual, violent, or toxic content) and apply similar precautions during data collection to minimize such content. We adhere to established research integrity practices, including reproducibility, transparency, and proper attribution of prior work.

O REPRODUCIBILITY STATEMENT

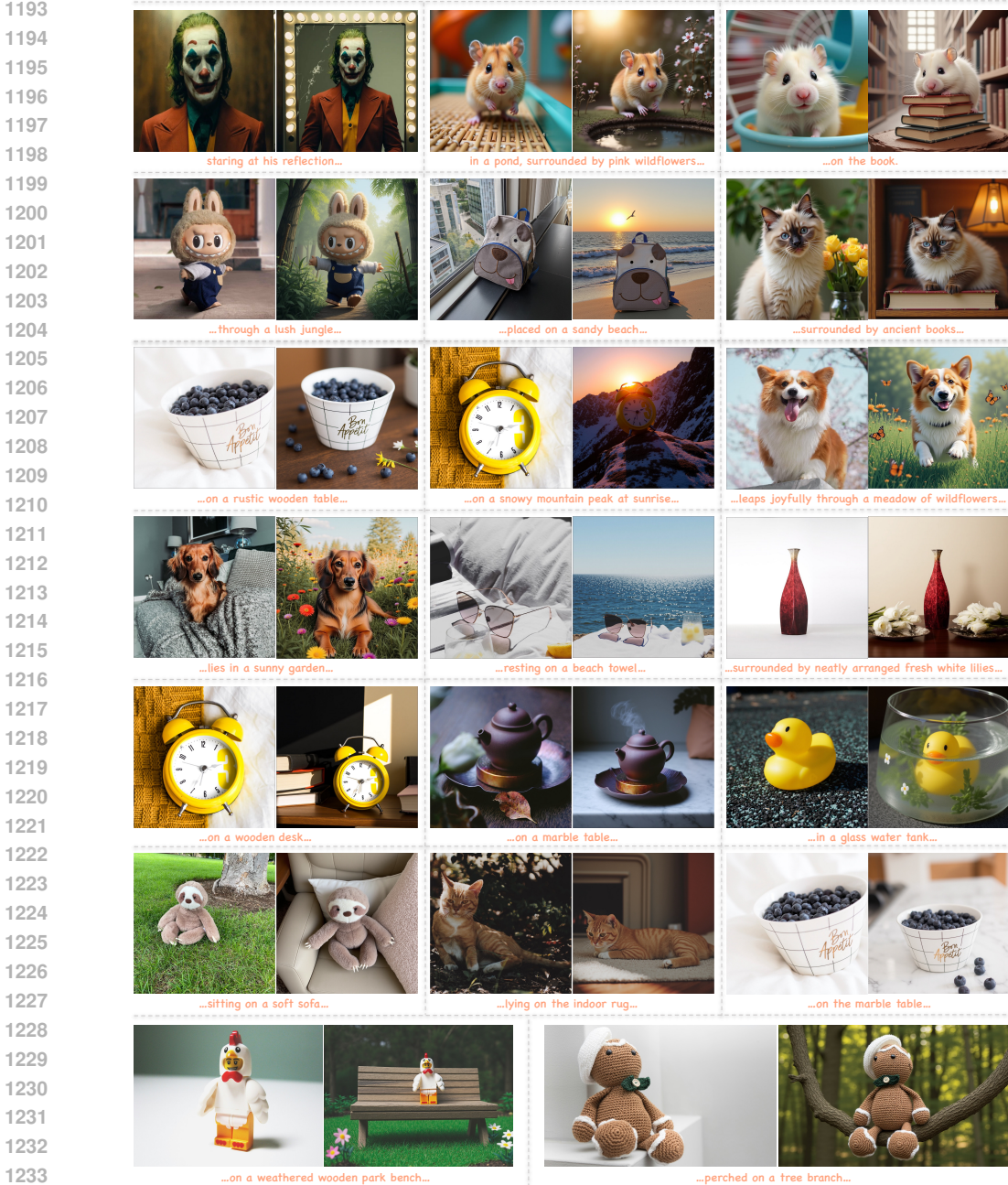
To ensure reproducibility, we provide detailed descriptions of our data preparation and processing in Sec. 3.3, and implementation details in Sec. 4.1, including training hyperparameters, evaluation protocols, and baselines clarification. In Appendix Sec. J, we also describe the prompts used when preparing data with the multi-modal language model. We will release our code and models under appropriate licenses to facilitate full reproducibility.

P LLM USAGE STATEMENT

In preparing this paper, we used large language models (LLMs), including ChatGPT (Hurst et al., 2024a) and Gemini (Team et al., 2023), solely as writing-assistance tools. Specifically, we first drafted the content ourselves and then used LLMs with prompts such as “You are an expert in academic writing. Please help me refine and rephrase the text to make it more professional, fluent,

³<https://iclr.cc/public/CodeOfEthics>

1188 clear, and readable.” We then manually reviewed and revised all LLM outputs to ensure that the text
 1189 accurately reflects our intended meaning. No part of the research design, experiments, analysis, or
 1190 results was generated by LLMs; their use was limited to improving clarity and readability of the
 1191 manuscript. We, the authors, take full responsibility for the content of this paper.
 1192



1235 **Figure 17: Additional visualization results on position-free customization.** Our method success-
 1236 fully maintains identity consistency while generating diverse scenes and poses.
 1237
 1238
 1239
 1240
 1241

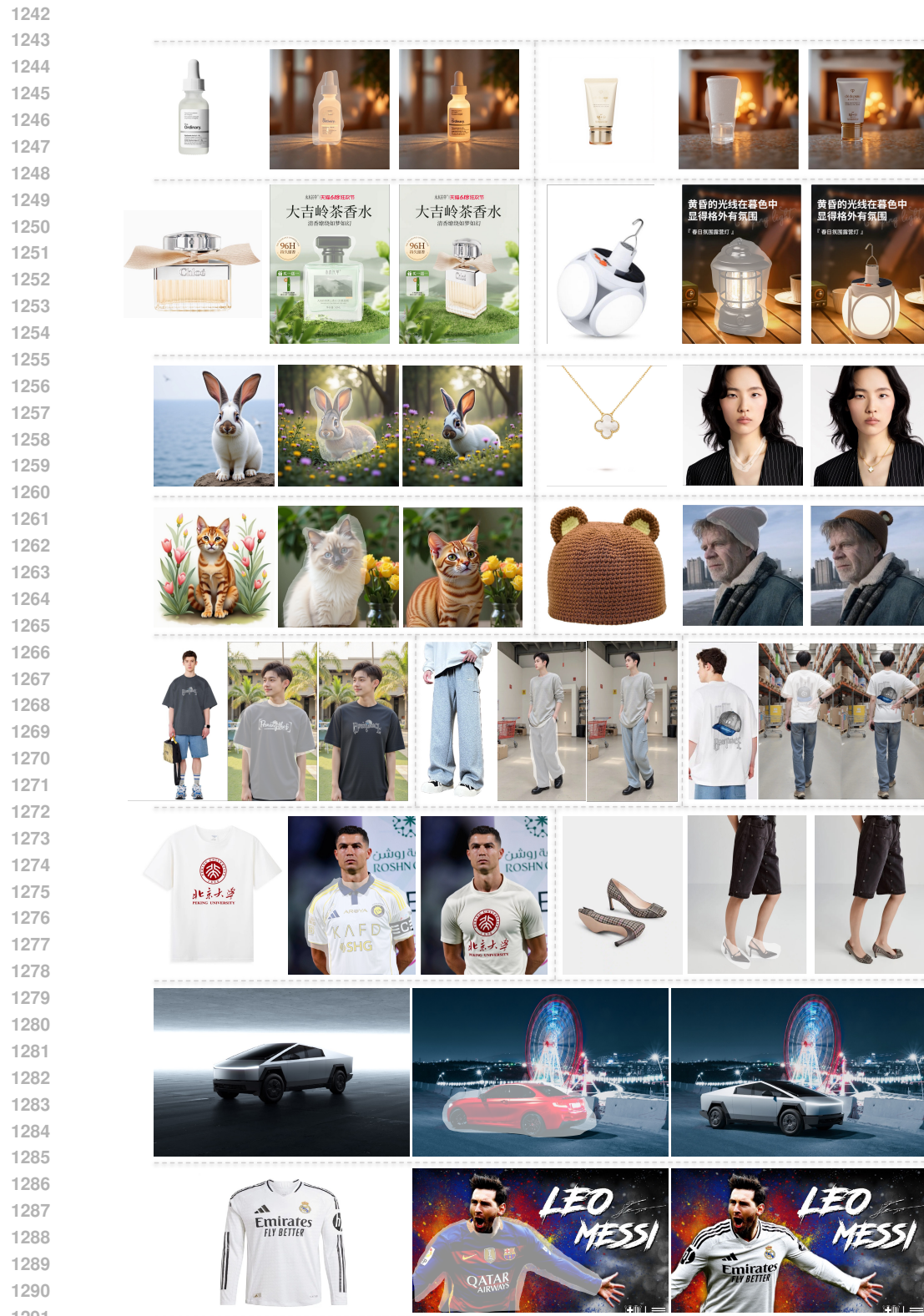


Figure 18: **Additional visualization results on position-aware customization.** Our method successfully maintains identity consistency while seamlessly integrating subjects into diverse lighting, styles, and poses in target scenes.

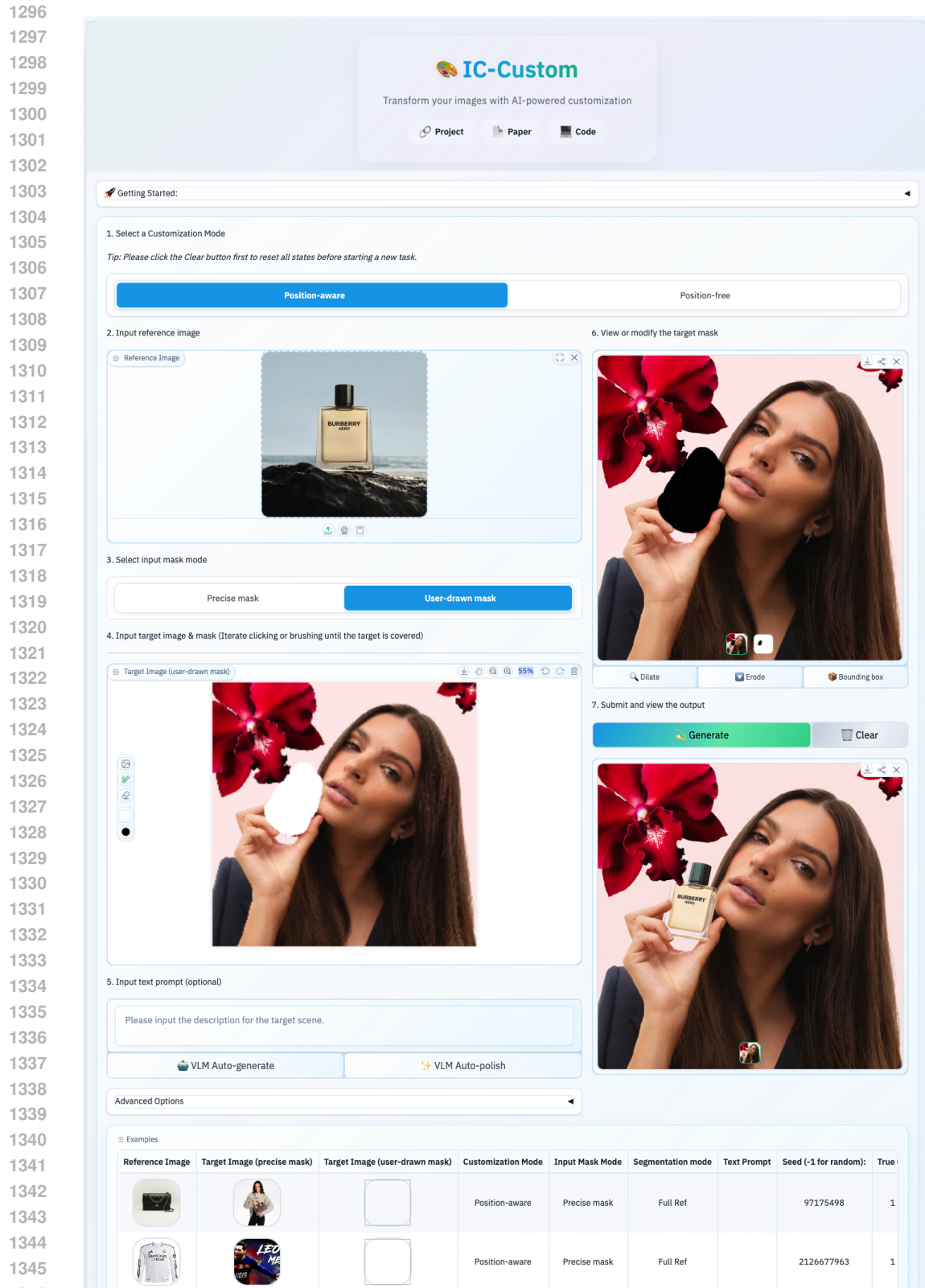


Figure 19: **Web App – Position-aware mode.** Users upload a reference image and a fill-in image, choose the mask type (precise or user-drawn), optionally edit or refine the mask, add an optional text prompt, and then run the model to perform position-aware customization.

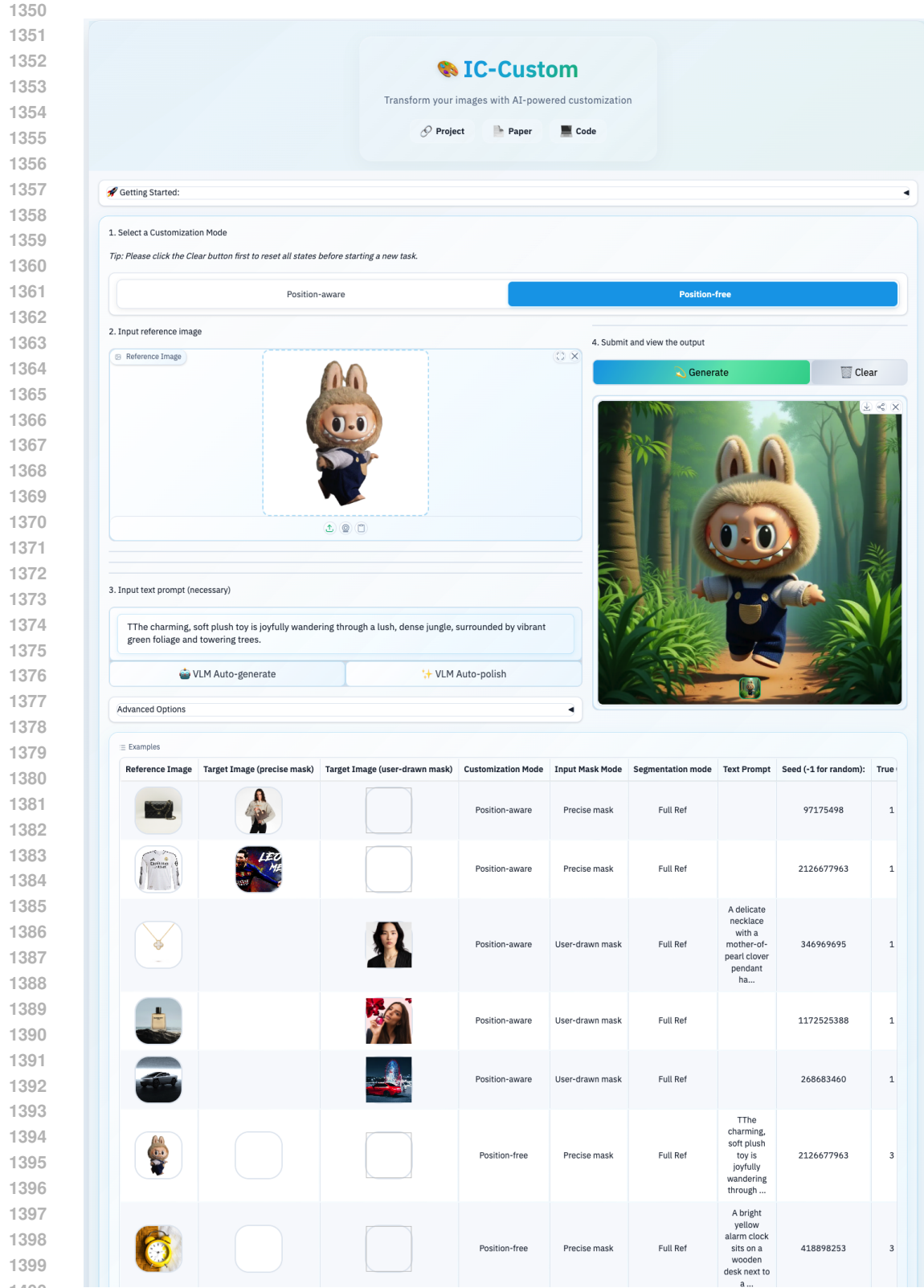


Figure 20: **Web App – Position-free mode.** Users upload a reference image, provide a text prompt describing the desired scene or use the built-in VLM prompt generator, and then run the model to perform position-free customization.